Dual magnetic correlations in filled skutterudite compound NdRu$_4$P$_{12}$

S. Masaki,[*] T. Mito,[†] and S. Wada

Graduate School of Sciences, Kobe University, Kobe 657-8501, Japan

H. Sugawara

Faculty of Integrated Arts and Sciences, The University of Tokushima, Tokushima 770-8502, Japan

D. Kikuchi and H. Sato

Graduate School of Science, Tokyo Metropolitan University, Hachioji, Tokyo 192-0397, Japan

We report the results of ^{31}P-nuclear magnetic resonance, ^{101}Ru-nuclear quadrupole resonance (NQR), and ac susceptibility (χ_{ac}) measurements on NdRu$_4$P$_{12}$. This compound is one of the filled skutterudite family RRu$_4$P$_{12}$ (R=rare earth) in which intimate relationships between $4f$ and conduction electrons with the nesting property of the Fermi surface may play an important role in a variety of intriguing low-temperature states. The NQR and χ_{ac} measurements indicate the appearance of ferromagnetic ordering below T_C=1.7 K. In the paramagnetic state, the coexistence of ferromagnetic and antiferro-type spin correlations are suggested from the field and temperature dependences of the Knight shift and the spin-lattice relaxation time. Such dual spin fluctuations can be explained by considering contributions from both localized $4f$ and conduction electrons with the nesting condition.

PACS number(s): 71.27.+a, 76.60.Gv

I. INTRODUCTION

The filled skutterudites RT_4X_{12}, with R=rare earth, T=Fe, Ru, and Os, and X=P, As, and Sb, have attracted considerable attention because of a variety of fascinating low-temperature states, such as unconventional heavy fermion state,[1,2] exotic superconductivity,[3] and multipolar ordering.[4–6] These properties may arise from the unique crystal structure of this family (space group $Im\bar{3}$); a cage formed by twelve X atoms surrounding an R ion is responsible for hybridization between f and conduction electrons, and the multipolar degrees of freedom can remain due to the highly symmetric cubic structure.

Among the filled skutterudites, a series of RRu$_4$P$_{12}$ reveals intriguing properties in which the nesting condition of the Fermi surface plays a key role. For R=La compound, the band calculation study and the de Haas–van Alphen (dHvA) experiment indicate the nesting properties of the Fermi surface with $q=(1,0,0)$.[7,8] R=Pr and Sm compounds undergo metal-insulator (M-I) transitions at 63 and 16.5 K, respectively.[9,10] The origin of the transitions is explained by the occurrence of some antiferro-type order; doubling the unit-cell size at half filling can wipe out the whole carriers. Indeed, it was found that below the transition temperatures the body-centered-cubic (bcc) crystal structure of the filled skutterudites changes to the structure where there are two inequivalent R sites (R=Pr or Sm) characterized by the wave vector $q=(1,0,0)$ (Ref. 11) as evidenced by the diffraction measurements for PrRu$_4$P$_{12}$ (Refs. 12–14) and the nuclear quadrupole resonance (NQR) measurement for SmRu$_4$P$_{12}$.[15] For R=Gd and Tb compounds, they also exhibit a remarkable increase in the electric resistivity below about 20 K accompanied with antiferromagnetic (AFM) ordering.[16] By considering that LaRu$_4$P$_{12}$ does not show the M-I transition, those transport anomalies are attributed to the cooperative

effect between the degrees of the R-$4f$ electrons and the nesting property of the Fermi surface.

In order to gain more insight into the role of R-$4f$ and conduction electrons, we have investigated isostructural relative NdRu$_4$P$_{12}$. The dHvA effect measurement on this compound indicates the similarity of the topology of the Fermi surfaces to those of LaRu$_4$P$_{12}$, implying that NdRu$_4$P$_{12}$ also has a good nesting condition of the Fermi surface and that Nd-$4f$ electrons are well localized.[17] Effective moment of $3.68\mu_B$ estimated from the temperature dependence (100 to 300 K) of the inverse dc susceptibility, $1/\chi_{dc}$, is close to the full free-ion moment of Nd^{3+}, $3.62\mu_B$, consistent with the well localized character of $4f$ electrons.[17] The electrical resistivity behaves as metallic above $\sim$10 K. It shows $-\ln T$ such as dependence below 10 K instead of the marked increase observed in R=Pr, Sm, Gd, and Tb compounds.[9,10,16] Below $T_C^{\rho} \sim 1.7$ K, the resistivity of NdRu$_4$P$_{12}$ rapidly decreases,[17] which resembles that of NdFe$_4$P$_{12}$.[18] Because T_C^{ρ} increases with increasing magnetic field, it is conjectured that ferromagnetic (FM) ordering appears below this temperature.

In this paper, we report the results of ^{31}P-nuclear magnetic resonance (NMR), ^{101}Ru-NQR, and ac susceptibility (χ_{ac}) measurements on NdRu$_4$P$_{12}$. The NQR and the NMR measurements at the different sites give the site-dependent microscopic information about static and dynamical magnetic properties. Besides, the NQR measurements in zero field and the NMR at various fields allow one to investigate the field dependence of spin correlations systematically

In the present study, the χ_{ac} and NQR studies confirmed the appearance of FM ordering below T_C=1.7 K in NdRu$_4$P$_{12}$. In the paramagnetic state, the Knight shift and the spin-lattice relaxation-time T_1 measurements indicate the coexistence of the FM spin correlation of $q=0$ and the antiferro-type correlation of $q \neq 0$. The origin of these dual spin fluctuations can be explained by considering contribu-

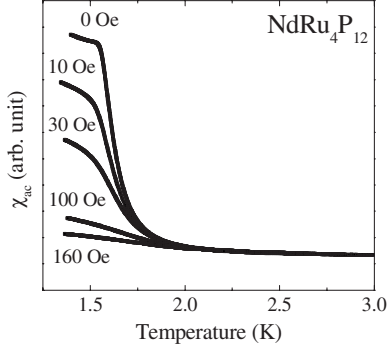FIG. 1. Temperature dependence of the ac susceptibility χ_{ac} at 0, 10, 30, 100, and 160 Oe in NdRu$_4$P$_{12}$.

FIG. 2. (Color online) Temperature dependence of the ^{101}Ru-NQR spectrum for the $\pm 1/2 \leftrightarrow \pm 3/2$ transition below 4.2 K. The spectrum intensity I is multiplied by temperature T.

tions from both localized 4f and conduction electrons with the nesting property of the Fermi surface.

II. EXPERIMENTAL DETAILS

Single crystals were synthesized by a tin flux method and by using 3N-Nd, 4N-Ru, 6N-P, and 5N-Sn. The detail of sample preparation was described in Ref. 19. The single-crystal pieces were ground into powder with the size of a few hundred microns. The ^{31}P-NMR and ^{101}Ru-NQR measurements were carried out by using the spin-echo technique with a phase-coherent pulsed spectrometer. The NMR lines were obtained by sweeping magnetic field at the different frequencies of 5.1711, 21.3701, and 51.711 MHz. The NQR spectrum measurements were performed as a function of frequency in zero field. The T_1 measurements using a single rf-pulse saturation method were carried out by the ^{31}P-NMR and the ^{101}Ru-NQR experiments. $^{31}T_1$ for the ^{31}P site was evaluated by fitting the decay curves to a single exponential function. $^{101}T_1$ measured at the $\pm 3/2 \leftrightarrow \pm 5/2$ level transition was obtained by fitting the data to the relaxation function given by

$$\frac{M(\infty) - M(t)}{M(\infty)} = \frac{3}{7}\exp\left(-\frac{3}{T_1}t\right) + \frac{4}{7}\exp\left(-\frac{10}{T_1}t\right).$$

The $^{101}T_1$ decay curves were well fit with a single component in the whole temperature range. However, $^{31}T_1$ was not uniquely determined at low temperatures as described later. The temperature and field dependences of the χ_{ac} were obtained by measuring the inductance of a coil with the sample inside at the frequency of 4kHz. The dc susceptibility (χ_{dc}) was measured by using a Quantum Design superconducting quantum interference device (SQUID) magnetometer.

III. RESULTS AND DISCUSSION

Figure 1 exhibits the temperature dependence of the χ_{ac} at different fields. The zero field χ_{ac} shows a rapid increase below 2 K and a kink at T_C=1.7 K, suggesting the appearance of magnetic ordering in NdRu$_4$P$_{12}$ below T_C. The enhancement of the χ_{ac} at low temperatures is largely suppressed by applying field of several tens oersted. This behavior is a characteristic of FM ordering, namely, a single
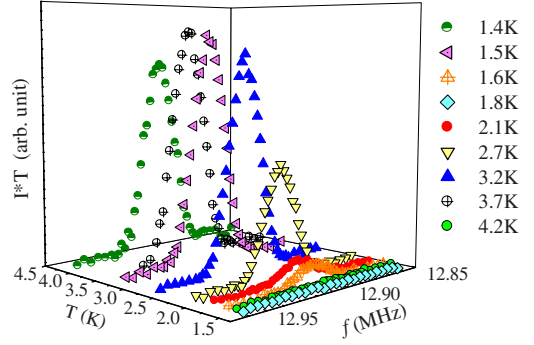
FM domain structure is formed by such small fields. Thus, the results of the χ_{ac} indicate that the ground state of this compound is a FM ordering state.

The emergence of spontaneous internal field due to the magnetic ordering was also evidenced by the ^{101}Ru-NQR experiment microscopically. The energy levels of the nuclear spin are generally determined by the next Hamiltonian,

$$\mathcal{H} = (h\nu_Q/6)[3I_z^2 - I^2 + \eta(I_x^2 - I_y^2)] - \gamma\hbar\boldsymbol{I}\cdot\boldsymbol{H}_{int}, \quad (1)$$

where the first term represents the electric quadrupole interaction between the nuclear quadrupole moment Q and the electric-field gradient (EFG) $V_{\alpha\alpha}$ at the nuclear position along the α direction. The nuclear spin I=5/2 for ^{101}Ru, ν_Q=3$eQV_{zz}/2I(2I+1)h$, and η=($V_{xx}-V_{yy})/V_{zz}$ following $V_{zz} \geq V_{xx} \geq V_{yy}$. The second term is the ordinary Zeeman effect caused by internal field $\boldsymbol{H}_{int}$ originating from the magnetic order. When $QV_{zz} \neq 0$ and $\boldsymbol{H}_{int}$=0, the nuclear-spin state with a sixfold degeneracy splits into three levels of $\pm 1/2$, $\pm 3/2$, and $\pm 5/2$. Then two resonance lines for $\pm 1/2 \leftrightarrow \pm 3/2$ and $\pm 3/2 \leftrightarrow \pm 5/2$ level transitions are observable.

Figure 2 shows the temperature dependence of the NQR spectrum multiplied by temperature for the $\pm 1/2 \leftrightarrow \pm 3/2$ transition. The sharp signal with the linewidth less than 20 kHz abruptly disappears below T_C without showing any broadening. This is explained by a modification in the resonance condition due to the appearance of spontaneous internal field $\boldsymbol{H}_{int}$. Such behavior is in contrast to the case of the ^{101}Ru-NQR spectrum measurement in SmRu$_4$P$_{12}$. This compound also undergoes magnetic ordering below 16.5 K, however, the ^{101}Ru-NQR spectrum in the ordered state is not influenced from the Zeeman effect at all.[15] This is because, although the microscopic mechanism of the order has not been clarified yet, the ordered structure in SmRu$_4$P$_{12}$ is characterized by an AFM wave vector $\boldsymbol{q}$=(1,0,0), leading $\boldsymbol{H}_{int}$ at the Ru sites to be canceled out due to a form factor. In this context, the observation of finite $\boldsymbol{H}_{int}$ in the present ^{101}Ru-NQR study is consistent with FM ordering in NdRu$_4$P$_{12}$.

In order to investigate the field effect on the spin correlations, we have carried out ^{31}P-NMR measurements at different fields. The typical temperature dependence of the

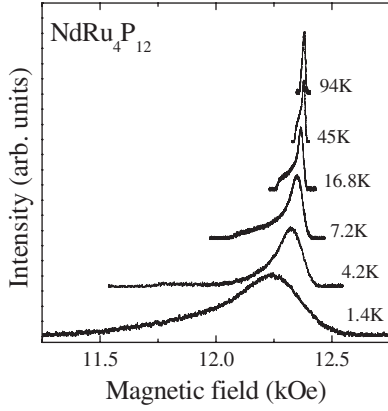FIG. 3. Temperature dependence of the ^{31}P-NMR spectrum measured at the frequency of 21.3701 MHz.

^{31}P-NMR spectrum is shown in Fig. 3. With decreasing temperature, the linewidth markedly increases and no clear anomaly is observed at T_C. These are because the FM transition becomes broadened under magnetic field and short-range FM order is induced even above T_C.

The line shape above 10 K is characteristic of a powder pattern structure for the nuclear spin $I=1/2$ with anisotropic hyperfine coupling constants. We here analyze the spectrum data using the parameters of the Knight shift perpendicular (parallel), $K_{\perp(\parallel)}$, to the principal axis by assuming an axial symmetry along the principal axis. Figure 4(a) shows the temperature dependences of $K_\perp$ and $K_\parallel$. Here, $K_\perp$ was determined from the maximum in the spectra and $K_\parallel$ was derived from the derivation of the shoulder peak in the spectra, as shown in the inset of Fig. 4(a). Because the shoulder peak becomes too indistinct at low temperatures to determine $K_\parallel$, we plot only the data above 10 K in Fig. 4(a). Besides, $K_\perp$ is field dependent below ~ 5 K, which is attributed to the field-induced short-range FM order. On the other hand, $K_\parallel$ and $K_\perp$ above 10 K are almost independent of field, which is contrary to the results of $1/T_1$ as described later.

Both $K_\perp$ and $K_\parallel$ monotonically increase as temperature decreases. The Knight shift is generally related to χ_{dc} as follows:

$$K_i = (A_i/N_A\mu_B)\chi_{dc}, \qquad (2)$$

where A_i ($i=\perp$ and $\parallel$) is the hyperfine coupling constant, and N_A is the Avogadro number. χ_{dc} is expressed as $\chi'(0,0)$, where $\chi'(q,\omega)$ is the real part of the dynamical susceptibility $\chi(q,\omega)$. The Knight-shift data hence provide useful information about the $q=0$ component of $\chi(q,\omega)$. In Fig. 4(b), we plot K_i versus χ_{dc} only above 10 K. Here, we used the χ_{dc} data measured at the field of 12.4 kOe for a polycrystalline sample because, in this temperature region, χ_{dc} is almost independent of field from the measurements up to 70 kOe as well as the Knight shift.[17] Besides, χ_{dc} is almost isotropic above 10 K. The linear relation is clearly seen between K_i and χ_{dc}. $A_\perp$ and $A_\parallel$ are evaluated to be 0.16 ± 0.01 and 1.21 ± 0.01 kOe/μ_B, respectively. These values are well understood in terms of the isotropic positive hyperfine field plus the anisotropic dipole-dipole couplings between Nd lo-
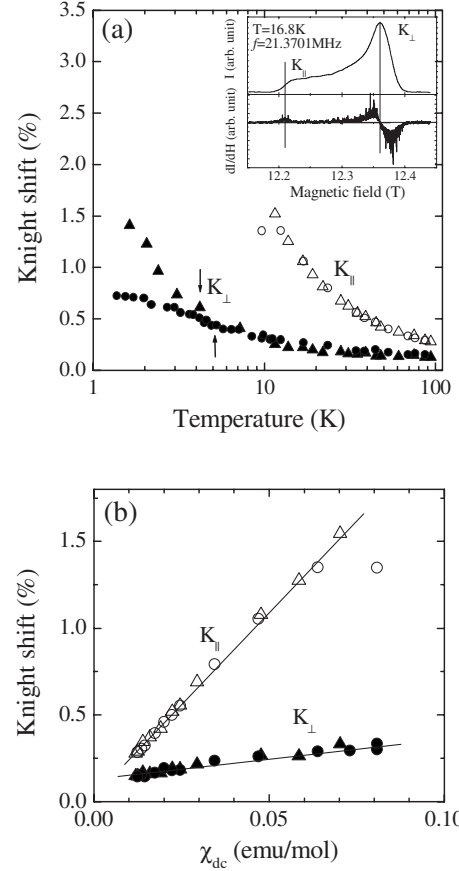

FIG. 4. (a) Temperature dependence of the Knight shifts, $K_\perp$ and $K_\parallel$, measured at ~ 12.4 (triangles) and ~ 30.0 kOe (circles) on a semilogarithmic scale. The down and up arrows indicate the temperatures where $^{31}(1/T_1T)$ shows a maximum at ~ 12.4 and ~ 30.0 kOe, respectively [see the inset of Fig. 5(a)]. The inset shows a representative NMR spectrum (upper line) and its derivation as a function of field. The data were obtained at 16.8 K and 21.3701 MHz. (b) $K_\perp$ and $K_\parallel$ versus χ_{dc} plots with temperature as an implicit parameter. The Knight-shift data were measured at the fields of ~ 12.4 (triangles) and ~ 30.0 kOe (circles), and only the data above 10 K were plotted.

cal moments and a given P nucleus. The isotropic term may arise from polarized P-3s electrons through the hybridization between P-3s and Nd-4f orbitals.

Next, we will show the results of T_1 measurements for the ^{31}P and ^{101}Ru sites. T_1 is generally described as follows:

$$\frac{1}{T_1} = \frac{2\gamma_N^2 k_B T}{(\gamma_e \hbar)^2} \sum_q A_q^2 \frac{\chi''(q,\omega_0)}{\omega_0}. \qquad (3)$$

Here, $A(q)$ is the q-dependent hyperfine coupling constant. $\chi''(q,\omega)$ is the imaginary part of $\chi(q,\omega)$ and is intimately related to $\chi'(q,\omega)$ through the Kramers-Kronig relation. NMR frequency ω_0 is of the order 5–50 MHz for the present study, which corresponds to the energy scale of $\hbar\omega_0 \sim 0.25$–2.5 mK. Therefore one can be regarded as $\omega_0 \rightarrow 0$.

The temperature dependences of T_1 for both sites are summarized in Fig. 5(a) ($1/T_1T$ vs T) and Fig. 5(b) ($1/T_1$ vs T). For the ^{31}P site, $^{31}(1/T_1T)$ measured at ~ 3 kOe is
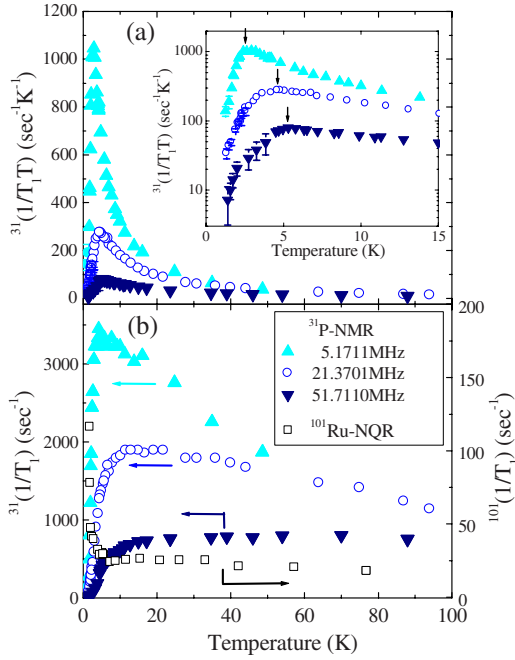
FIG. 5. (Color online) (a) Temperature dependence of $^{31}(1/T_1T)$ measured by ^{31}P-NMR measurement at different frequencies $\omega/2\pi=5.1711$ MHz (~3.0 kOe), 21.3701 MHz (~12.4 kOe), and 51.711 MHz (~30.0 kOe). Inset: Temperature dependences of $^{31}(1/T_1T)$ on a semilogarithmic scale in the low-temperature region below 15 K. The arrow shows the temperature where $^{31}(1/T_1T)$ is a maximum. The error bars for $^{31}(1/T_1T)$ at low temperatures represent the distribution of $^{31}T_1$. (b) Temperature dependence of $^{31}(1/T_1)$ (left axis) and $^{101}(1/T_1)$ obtained by the ^{101}Ru-NQR measurement (right axis).

largely enhanced with decreasing temperature [see the up triangles in Fig. 5(a)], implying the significant development of the low-energy spin fluctuations. As further decreasing temperature, $^{31}(1/T_1T)$ decreases with a peak around 2.5 K. Because this peak shifts to higher temperature with increasing field as indicated by the arrows in the inset of Fig. 5(a), the drop of $^{31}(1/T_1T)$ is attributed to the suppression of FM spin fluctuations. Note that the shift of the peak (2.5 K at 3 kOe to 5 K at 30 kOe) reasonably corresponds to the Zeeman energy of the applied fields. The Knight shift, namely $\chi'(0,0)$, is inevitably dependent on field below the temperatures indicated by the arrows, as shown in Fig. 4(a). In this temperature region, the $^{31}T_1$ decay curve deviates from the single exponential function, which is attributed to inhomogeneous internal field due to the field-induced short-range FM order. The distribution of T_1 is exhibited by the error bars in the inset of Fig. 5(a).

The magnetic order is also evidenced by a steep increase in $^{101}(1/T_1)$ for the ^{101}Ru site down to ~2 K, the lowest temperature where the ^{101}Ru-NQR signal is observable [see the open squares in Fig. 5(b)]. This is the so called "critical slowing down behavior," i.e., the T_1 relaxation rate divergently increases when the spin fluctuation energy crosses $\hbar\omega_0$ around magnetic ordering temperature. Here, $^{101}T_1$ data reflect the temperature dependence of the $q\sim0$ component of $\chi(q,\omega)$, as discussed below.

The features of the field and temperature dependences of T_1 are summarized as follows: (i) $^{31}(1/T_1)$ for the P site is drastically suppressed with increasing field. Surprisingly, this field effect reaches to ~100 K under 30 kOe [see Fig. 5(b)], which may be distinguished from the above-mentioned suppression of the FM spin fluctuations below ~5 K. $^{31}(1/T_1)$ measured at ~30 kOe does not depend on temperature above 10 K. (ii) $^{101}(1/T_1)$ measured by the ^{101}Ru-NQR is almost independent of temperature above 10 K, which is analogous with the $^{31}(1/T_1)$ data measured at 30 kOe [see Fig. 5(b)].

In the following, we will discuss the properties of low-energy spin fluctuations above 10 K. In this temperature region, the Knight shift little depends on field as shown in Fig. 4(a), implying that $\chi'(0,0)$ is not sensitive to field. Therefore the field dependent part of the spin fluctuations, which causes the significant enhancement of $^{31}(1/T_1T)$ at low fields and low temperatures, are dominated by $\chi(q\neq0,\omega_0)$. The results of (ii) indicates that this field sensitive component with $q\neq0$ is effectively small at the Ru site even in zero field. This is explained by assuming that the $q\neq0$ components are dominated by $\chi(Q)$, where the AFM wave vector $Q=(1,0,0)$. Namely, spin fluctuation with $Q=(1,0,0)$ would be canceled out at the Ru site due to a form factor since the Ru ions are located at the middle between two Nd sites. In fact, such an effect of the form factor at the Ru site is observed in the ordered state of SmRu$_4$P$_{12}$ as mentioned before.[15] Thus, in addition to the different field dependence between the Knight shift and T_1, the different temperature dependence of T_1 between the P and Ru sites at high temperatures will be well explained by the coexistence of the spin fluctuations with $q=0$ and $q\neq0$.

The $T_1\sim$ const behavior, which is seen in the ^{31}P-NMR at 30 kOe and ^{101}Ru-NQR, is known to be the characteristic temperature dependence when the T_1 relaxation process is dominated by the spin fluctuations of localized moments. Therefore the FM correlation may originate from localized Nd-4f electrons.

To understand the dual magnetic correlations in NdRu$_4$P$_{12}$, the nesting property of conduction electrons, which is common in RRu$_4$P$_{12}$ systems, may provide a hint. The antiferro-type correlation will be favorable for the nesting condition. If the wave vector of the magnetic or electric correlation coming from the localized 4f electrons coincides with the nesting vector, the two properties will be cooperative. Then the resulting transition temperature will be relatively high. This is the case for PrRu$_4$P$_{12}$ (Refs. 5 and 14) and SmRu$_4$P$_{12}$.[15] The clear increase in the resistivity, accompanied with the AFM order, in TbRu$_4$P$_{12}$ and GdRu$_4$P$_{12}$ are also consistent with this scheme. On the other hand, the nesting property will compete with the FM correlation in NdRu$_4$P$_{12}$. This may lead to much lower transition temperature than those of the antiferro-type orders mentioned above. It is, however, unlikely that such a simple model satisfactorily explains the unusually strong-field dependence observed in the present ^{31}P-NMR experiments, namely, the field effect on $^{31}(1/T_1)$ caused by 30 kOe reaches to 100 K. In order to clarify this problem, it will be necessary to uncover more detailed q dependence of magnetic correlations, for example, by inelastic neutron-scattering experiments.

IV. CONCLUSIONS

We have shown that ferromagnetism arises in $NdRu_4P_{12}$ at $T_C = 1.7$ K by the ac χ and ^{101}Ru-NQR spectrum measurements. Besides, the field and temperature dependences of the Knight shift and T_1, which were obtained by ^{31}P-NMR and ^{101}Ru-NQR measurements, suggest that the FM spin correlation coexists with the antiferro-type fluctuation of $q \neq 0$. In order to explain such dual spin fluctuations, one may need to consider the intimate relationship between localized $4f$ and conduction electrons with the nesting property of the Fermi surface, as suggested in other RRu_4P_{12} compounds as well.

*s-masaki@stu.kobe-u.ac.jp

[†]Present address: Graduate School of Material Science, University of Hyogo, Hyogo 678-1297, Japan.

[1] Y. Aoki, T. Namiki, T. D. Matsuda, K. Abe, H. Sugawara, and H. Sato, Phys. Rev. B **65**, 064446 (2002).

[2] S. Sanada, Y. Aoki, H. Aoki, A. Tsuchiya, D. Kikuchi, H. Sugawara, and H. Sato, J. Phys. Soc. Jpn. **74**, 246 (2005).

[3] E. D. Bauer, N. A. Frederick, P.-C. Ho, V. S. Zapf, and M. B. Maple, Phys. Rev. B **65**, 100506(R) (2002).

[4] Y. Aoki, T. Namiki, T. D. Matsuda, H. Sugawara, and H. Sato, J. Phys. Chem. Solids **63**, 1201 (2002).

[5] T. Takimoto, J. Phys. Soc. Jpn. **75**, 034714 (2006).

[6] M. Yoshizawa, Y. Nakanishi, M. Oikawa, C. Sekine, I. Shirotani, S. R. Saha, H. Sugawara, and H. Sato, J. Phys. Soc. Jpn. **74**, 2141 (2005).

[7] H. Harima and K. Takegahara, Physica B **312-313**, 843 (2002).

[8] S. R. Saha, H. Sugawara, Y. Aoki, H. Sato, Y. Inada, H. Shishido, R. Settai, Y. Onuki, and H. Harima, Phys. Rev. B **71**, 132502 (2005).

[9] C. Sekine, T. Uchiumi, I. Shirotani, and T. Yagi, Phys. Rev. Lett. **79**, 3218 (1997).

[10] C. Sekine, T. Uchiumi, I. Shirotani, and T. Yagi, in *Science and Technology of High Pressure*, edited by M. H. Manghnant and M. F. Nocol (Universities Press, Hyderabad, 2000), p. 826.

[11] In the ordered state, the center and corner R atoms in the bcc structure occupy different sublattices.

[12] C. H. Lee, H. Matsuhata, A. Yamamoto, T. Ohta, H. Takazawa, K. Ueno, C. Sekine, I. Shirotani, and T. Hirayama, J. Phys.: Condens. Matter **13**, L45 (2001).

[13] C. H. Lee, H. Matsuhata, H. Yamaguchi, C. Sekine, K. Kihou, T. Suzuki, T. Noro, and I. Shirotani, Phys. Rev. B **70**, 153105 (2004).

[14] K. Iwasa, L. Hao, T. Hasegawa, T. Takagi, K. Horiuchi, Y. Mori, Y. Murakami, K. Kuwahara, M. Kohgi, H. Sugawara, S. R. Saha, Y. Aoki, and H. Sato, J. Phys. Soc. Jpn. **74**, 1930 (2005).

[15] S. Masaki, T. Mito, M. Takemura, S. Wada, H. Harima, D. Kikuchi, H. Sato, H. Sugawara, N. Takeda, and G.-q. Zheng, J. Phys. Soc. Jpn. **76**, 043714 (2007).

[16] C. Sekine, T. Uchiumi, I. Shirotani, K. Matsuhira, T. Sakakibara, T. Goto, and T. Yagi, Phys. Rev. B **62**, 11581 (2000).

[17] H. Sugawara *et al.* (unpublished).

[18] H. Sugawara, Y. Abe, Y. Aoki, H. Sato, M. Hedo, R. Settai, Y. Onuki, and H. Harima, J. Phys. Soc. Jpn. **69**, 2938 (2000).

[19] W. Jeitschko and D. J. Braun, Acta Crystallogr., Sect. B: Struct. Crystallogr. Cryst. Chem. **33**, 3401 (1977).